Contents lists available at ScienceDirect

Epidemics

Check for updates

Policy-driven mathematical modeling for COVID-19 pandemic response in the Philippines

Elvira de Lara-Tuprio [a], Carlo Delfin S. Estadilla [a], Jay Michael R. Macalalag [b],
Timothy Robin Teng [a], Joshua Uyheng [c,*], Kennedy E. Espina [d], Christian E. Pulmano [d],
Maria Regina Justina E. Estuar [d], Raymond Francis R. Sarmiento [e]

[a] *Department of Mathematics, Ateneo de Manila University, Philippines*
[b] *Department of Mathematics, Caraga State University, Philippines*
[c] *Department of Psychology, Ateneo de Manila University, Philippines*
[d] *Department of Information Systems and Computer Science, Ateneo de Manila University, Philippines*
[e] *National Institutes of Health, University of the Philippines Manila, Philippines*

A B S T R A C T

Around the world, disease surveillance and mathematical modeling have been vital tools for government responses to the COVID-19 pandemic. In the face of a volatile crisis, modeling efforts have had to evolve over time in proposing policies for pandemic interventions. In this paper, we document how mathematical modeling contributed to guiding the trajectory of pandemic policies in the Philippines. We present the mathematical specifications of the FASSSTER COVID-19 compartmental model at the core of the FASSSTER platform, the scenario-based disease modeling and analytics toolkit used in the Philippines. We trace how evolving epidemiological analysis at the national, regional, and provincial levels guided government actions; and conversely, how emergent policy questions prompted subsequent model development and analysis. At various stages of the pandemic, simulated outputs of the FASSSTER model strongly correlated with empirically observed case trajectories (r = 94%–99%, p < .001). Model simulations were subsequently utilized to predict the outcomes of proposed interventions, including the calibration of community quarantine levels alongside improvements to healthcare system capacity. This study shows how the FASSSTER model enabled the implementation of a phased approach toward gradually expanding economic activity while limiting the spread of COVID-19. This work points to the importance of locally contextualized, flexible, and responsive mathematical modeling, as applied to pandemic intelligence and for data-driven policy-making in general.

1. Introduction

The global COVID-19 pandemic represents one of the greatest public health crises in modern history (Cattani, 2020). Major efforts to contain outbreaks worldwide have utilized mathematical modeling to guide researchers, epidemiologists, and public health officials in understanding the nature of the disease, as well as evaluate potential measures to curb its spread (Boccaletti et al., 2020; Currie et al., 2020; Prem et al., 2020). Compartmental models, for instance, have been particularly popular for estimating key properties of the disease, forecasting epidemiological outcomes across different contexts and conditions, and evaluating the impacts of different interventions including targeted government lockdown scenarios, travel restrictions, or collective mask-wearing (Eikenberry et al., 2020; Lin et al., 2020b,a; Wynants et al., 2020).

With the explosion of mathematical modeling efforts to aid in pandemic response around the world (Gnanvi et al., 2021; Rahimi et al., 2021; Syeda et al., 2021), the goal of this paper is two-fold. First, we describe the mathematical details of the compartmental model which contributed to the pandemic response in the Philippines. As a developing country, the Philippines faces major economic constraints on available resources, indicating the urgent need for an enhanced understanding of local outbreak dynamics and capacity-building for harnessing data-driven insights (Dahab et al., 2020; Figueroa et al., 2021; McMahon et al., 2020). In this resource-scarce context, this paper's second goal is thus to trace how modeling efforts were used to directly guide local policy-making at multiple levels of governance

and decision-making. In this process, we conversely examine how emergent policy questions prompted subsequent improvements in model development and analysis.

Through this case study, we add to the ever-growing global literature on the use of mathematical models across different national contexts. But more specifically, we demonstrate how mathematical models are informed by the concrete settings in which they are utilized, and must flexibly evolve to address shifting policy needs (Bedford et al., 2020; DebRoy et al., 2017). As we later explain in detail, the interlocking development of mathematical modeling and policy-making pertains both to retrospective assessments of past interventions, as well as prospective scenario-based forecasts of future policy outcomes. By showing the interrelationships between mathematical modeling and context-specific policy-making concerns, we highlight novel, interdisciplinary contributions to the literature with implications for pandemic intelligence and general crisis informatics that extend beyond the Philippine example.

In the Philippines, the FASSSTER scenario-based disease modeling and analytics toolkit has contributed to the pandemic policy-making at multiple levels of governance.[1] The platform is a scenario-based disease modeling and surveillance platform developed for the Department of Health's Epidemiology Bureau (DOH-EB). The technologies embedded in the FASSSTER platform have previously been tested and utilized for localized monitoring of other infectious diseases such as dengue, measles, and typhoid (Espina and Estuar, 2017; Uyheng et al., 2020, 2018).

Coinciding with the World Health Organization's (WHO) declaration of COVID-19 as a pandemic, the Philippine Department of Health confirmed its first local case of COVID-19 in the first week of March 2020. At this time, FASSSTER was reconfigured to aid in the pandemic intelligence response in the Philippines (Estuar et al., 2020). With the development and deployment of the mathematical model of FASSSTER for the COVID-19 transmission in the Philippines, hereafter referred to as *the FASSSTER model*, public health policies in the country have been formulated with the guidance of data-driven inputs. Over the following year and into the time of writing, the FASSSTER model has guided both national and local governments in coordinating regional levels of mobility restrictions while expanding healthcare system capacity since the imposition of a strict enhanced community quarantine (ECQ) in March 2020 (Vallejo and Ong, 2020).

In the succeeding sections of this paper, we unpack the policy-driven design, deployment, and dynamic evolution of the FASSSTER model in the Philippines as follows. First, we present a description of the model formulation, its associated parameters, and their corresponding estimation procedures in Section 2. Second, we narrate in Section 3 how the model was utilized for answering particular policy questions, while also being adapted in line with shifting pandemic conditions. Finally, we discuss implications of the Philippine experience in data-driven pandemic response in Section 4. In sum, this work thus seeks to answer the following research questions:

1. How was mathematical modeling used to understand and forecast the COVID-19 case trajectories in the Philippines?
2. How did localized compartmental models guide policy decisions for the Philippine pandemic response?
3. How did mathematical models for pandemic intelligence evolve in response to changing policy needs in the Philippines?

---

[1] FASSSTER stands for Feasibility Analysis on Syndromic Surveillance using Spatio-Temporal Epidemiological modeleR, accessible online at https://fassster.ehealth.ph/covid19/.

2. The FASSSTER model of COVID-19

2.1. Model formulation

The FASSSTER model (Estadilla et al., 2021) is formulated as a compartmental model that traces the dynamics of COVID-19 infections throughout the Philippine population. Here, the population is divided into six compartments: susceptible (S), exposed (E), infectious but asymptomatic (I_a), infectious and symptomatic (I_s), confirmed (C), and recovered (R).

Following standard nomenclature (Eikenberry et al., 2020; Lin et al., 2020b,a; Wynants et al., 2020), compartment S consists of individuals who have not been infected with COVID-19 and may potentially become infected. Compartment E consists of individuals who have been infected but are not yet infectious. Both compartments I_a and I_s consist of individuals who are infectious but not yet confirmed clinically or documented. Compartment C consists of confirmed infected individuals who are assumed to be undergoing treatment and isolated so as not to infect those in the susceptible compartment. This compartment also represents the *active cases* in the community, and the goal is for the model output in C to capture this local case data. Lastly, compartment R consists of individuals from compartment C who have recovered from the disease. Although there have been major accounts that reinfection could occur (Gousseff et al., 2020; Stokel-Walker, 2021), the present model assumes that those who have recovered from the disease have acquired immunity and cannot infect others nor be reinfected anymore.

Fig. 1 (Estadilla et al., 2021) graphically illustrates population transitions between compartments as governed by the model parameters. Parameters include: the transmission rate β; the incubation period τ; the percentage ω of infectious asymptomatic individuals who eventually exhibit symptoms of the disease; the respective detection rates δ_a and δ_s of asymptomatic and symptomatic infectious individuals; and the respective recovery rates r and θ of confirmed and asymptomatic infectious individuals.

The transmission rate β is a function of the baseline disease transmission rate β_0, which is derived from an assumed basic reproduction number R_0, and a reduction factor $(1 - \lambda)$, where $\lambda \in [0, 1]$. In general, the parameter λ reflects several factors including the effect of community quarantine imposed by the government, as well as the compliance of the members of the population to minimum public health standards such as proper hygiene, social distancing, and the wearing of face masks and face shields. Infectiousness of asymptomatic relative to symptomatic cases is accounted for by the parameter ψ. The respective rates of transfer from exposed to infectious asymptomatic (α_a) and infectious symptomatic (α_s) compartments are derived using the incubation period parameter (τ) and the proportion of asymptomatic infections (c), where $\alpha_a = \frac{c}{\tau}$ and $\alpha_s = \frac{1-c}{\tau}$.

A constant recruitment rate A in the susceptible population is assumed, mainly through birth. Moreover, death due to causes other than COVID-19 is assumed to occur in all compartments at a rate μ per unit of time, also referred to as the natural death rate. Death due to the disease, on the other hand, is assumed to occur at the rates ϵ_I and ϵ_T per unit of time among the infectious symptomatic and confirmed cases, respectively.

Mathematically, the FASSSTER model is characterized by the following system of ordinary differential equations (Estadilla et al., 2021):

$$S'(t) = A - \frac{\beta S(t)}{N(t)} \left[\psi I_a(t) + I_s(t) \right] - \mu S(t) \tag{1}$$

$$E'(t) = \beta \frac{S(t)}{N(t)} \left[\psi I_a(t) + I_s(t) \right] - (\alpha_a + \alpha_s + \mu)E(t) \tag{2}$$

$$I_a'(t) = \alpha_a E(t) - (\omega + \delta_a + \theta + \mu)I_a(t) \tag{3}$$

$$I_s'(t) = \alpha_s E(t) + \omega I_a(t) - (\delta_s + \epsilon_I + \mu)I_s(t) \tag{4}$$

$$C'(t) = \delta_a I_a(t) + \delta_s I_s(t) - (r + \epsilon_T + \mu)C(t) \tag{5}$$

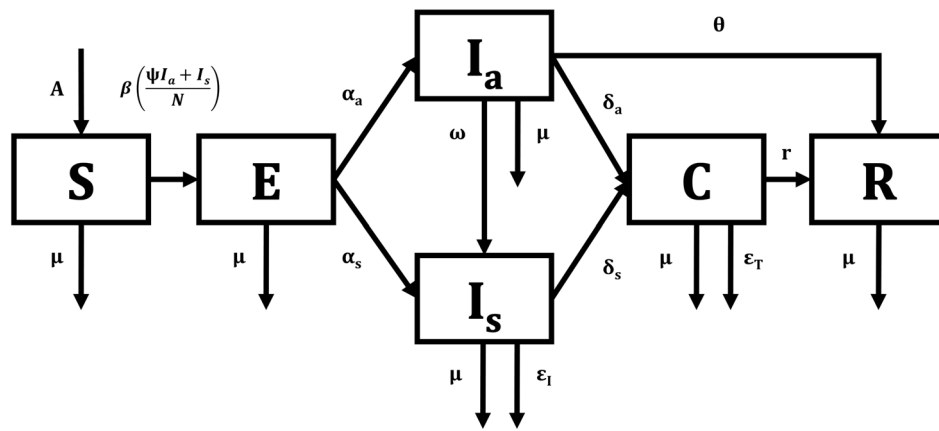$$R'(t) = rC(t) + \theta I_a(t) - \mu R(t), \tag{6}$$

Fig. 1. Diagram of the FASSSTER compartmental model. Disease progression from the susceptible (*S*) compartment through the exposed (*E*), asymptomatic (*I_a*) and symptomatic (*I_s*) infectious, confirmed (*C*), and recovered (*R*) compartments.

Table 1
Summary of parameter values and initial values of variables.

Variable	Description	Values/Source	Unit	References
Initial state values				
$S(0)$	Initial susceptible	population data	individuals	Philippine Statistics Authority (2020)
$E(0)$	Initial exposed	fitted	individuals	
$I_a(0)$	Initial infectious asymptomatic	fitted	individuals	
$I_s(0)$	Initial infectious symptomatic	fitted	individuals	
$C(0)$	Initial confirmed cases	actual data	individuals	Department of Health - Epidemiology Bureau (2020)
$R(0)$	Initial recovered	0	individuals	assumed
Model parameter values				
R_0	Basic reproduction number	4.0, 3.0	dimensionless	U.S. Centers for Disease and Control (2020)
A	Constant recruitment rate	population data	individuals/day	macrotrends (2020a), Philippine Statistics Authority (2020)
μ	Natural death rate	4.05×10^{-5}	1/day	macrotrends (2020b)
β_0	Baseline transmission rate	0.4343, 0.3258	1/day	U.S. Centers for Disease and Control (2020)
λ	Transmission reduction	fitted	1/day	
ψ	Relative infectiousness of asymptomatics	1.0000	dimensionless	U.S. Centers for Disease and Control (2020)
τ	Incubation period	5.0000	day	World Health Organization (2020b)
c	Proportion of asymptomatic infections	0.1800	dimensionless	Mizumoto et al. (2020)
ω	Symptomatic transition	0.3300	1/day	World Health Organization (2020a), Mizumoto et al. (2020)
θ	Undetected, asymptomatic recovery rate	0.0714	1/day	World Health Organization (2020b)
δ_a	Detection rate for asymptomatic	case data	1/day	Department of Health - Epidemiology Bureau (2020)
δ_s	Detection rate for symptomatic	case data	1/day	Department of Health - Epidemiology Bureau (2020)
r	Post-detection recovery rate	0.0404	1/day	Department of Health - Epidemiology Bureau (2020)
ϵ_I	COVID-19 death rate, undetected	0.0031	1/day	Department of Health - Epidemiology Bureau (2020)
ϵ_T	COVID-19 death rate, detected	0.0031	1/day	Department of Health - Epidemiology Bureau (2020)

where $\beta = \beta_0(1 - \lambda)$, $\alpha_a = \frac{c}{\tau}$, $\alpha_s = \frac{1-c}{\tau}$, and $N(t) = S(t) + E(t) + I_a(t) + I_s(t) + C(t) + R(t)$. The functions S, E, I_a, I_s, C, and R are differentiable real-valued functions on $\mathbb{R}$. All parameters are nonnegative constants.

2.2. Model parameters and initial state values

Compartmental models require numerical values of parameters as well as initial values for the state variables in order to project future dynamics of the disease. These parameters are determined for each locality—a city, municipality, province, or region—using three distinct strategies. First, some parameters were *calculated directly* from the case incidence data collected from the DOH-EB (Department of Health - Epidemiology Bureau, 2020). Others were *obtained from the literature* or existing databases with the exact measures needed for the model (macrotrends, 2020a,b; Philippine Statistics Authority, 2020). Lastly, to ensure that the output of the model was in line with the actual data, we implemented an *algorithmic fitting procedure*. This procedure was used to estimate the initial values $E(0)$, $I_a(0)$, $I_s(0)$. It was also used to calibrate λ periodically (Varadhan, 2014). Table 1 summarizes the parameter values and initial state values for the model.

2.2.1. Parameters estimated from local data and related studies

The FASSSTER model was designed to help national and local government units (LGU) in the Philippines understand the spread of disease in their locality and design appropriate interventions and policies. Hence, it was important to ensure that the output of the model was in line with their historical data of confirmed cases. This section summarizes our use of historical or literature values and direct calculation methods to obtain values of the model parameters.

To estimate the local recruitment rate *A*, the 2020 national birth rate (macrotrends, 2020a) was multiplied by the population size (Philippine Statistics Authority, 2020) of the locality. The natural death rate μ was obtained by getting the inverse of the national average life expectancy, given the absence of this statistic at the local level (macrotrends, 2020b).

The unit of time *t* is in days, with $t = 0$ corresponding to the first day after March 1 when a locality confirmed and admitted a COVID-19 case. Thus, $C(0)$ refers to the initial number of active cases in a given locality. Moreover, the initial susceptible population $S(0)$ in any locality was estimated as 75% of the local population at that time, following similar assumptions as in related work (Lin et al., 2020b).

Several parameters were obtained from the literature. WHO findings in Wuhan, China (World Health Organization, 2020b) have shown that

the average incubation period, τ, for COVID-19 may be approximately 5 days. The relative infectiousness of asymptomatic cases, ψ, remains highly uncertain. We conservatively assumed that $\psi = 1$, following the worst-case scenario considered by the US Centers for Disease and Control (U.S. Centers for Disease and Control, 2020). The proportion of asymptomatic infections, c, was fixed at 0.18, as found in a study of the spread of COVID-19 in the Diamond Princess cruise ship (Mizumoto et al., 2020), wherein 65% of asymptomatic cases developed symptoms later. Thus, the rate of transfer from exposed to infectious asymptomatic was $\alpha_a = \frac{0.18}{5}$ and the rate of transfer from exposed to infectious symptomatic was $\alpha_s = \frac{0.82}{5}$. Based on a WHO report (World Health Organization, 2020a) that it takes 2 days on average for an asymptomatic to develop symptoms, we estimated the rate of transfer, ω, from the asymptomatic (I_a) to the symptomatic compartment (I_s) to be equal to $\frac{1}{2} \times 0.65$. Lastly, we assume that it takes an average of 14 days for infectious asymptomatic cases to recover (World Health Organization, 2020b). Hence, the recovery rate θ of those in the I_a compartment who were never clinically diagnosed was estimated as $\frac{1}{14}$.

Some parameters were calculated and updated monthly from the data obtained from DOH-EB. These values were applied to all localities. The detection rate for symptomatic individuals, δ_s, was calculated by getting the inverse of the average number of days from the date of onset of symptoms to the report date. We then assumed that the detection rate for asymptomatic individuals, δ_a, is the same as δ_s. Note that this is a simplifying assumption because, in reality, symptomatic cases are more likely to get tested than asymptomatic cases. Nevertheless, for model output that focuses on projections of active cases or daily new cases, the current assumption should suffice. Next, the recovery rate r for confirmed cases was computed as the inverse of the average number of days from report date to the date of recovery. We also estimated the death rate due to COVID-19, ϵ_T and ϵ_I, by getting the average of the ratio of the reported number of deaths to the actual number of active cases per day based on local data.

Finally, the baseline disease transmission rate β_0 was obtained from the value of the basic reproduction number R_0. We assumed that $R_0 = 4$ for the National Capital Region (NCR), the Calabarzon Region, and Central Visayas Region, and $R_0 = 3$ for other regions. Using the next generation matrix approach, it can be shown that

$$R_0 = \frac{\beta[(\mu + \omega + \delta_a + \theta)\alpha_s + (\mu + \epsilon_I + \delta_s)\psi\alpha_a + \omega\alpha_a]}{(\mu + \omega + \delta_a + \theta)(\mu + \epsilon_I + \delta_s)(\mu + \alpha_a + \alpha_s)}.$$

By assigning the value 0 to λ at $t = 0$ so that $\beta = \beta_0$, then β_0 can be obtained from the above formula using the values of the other parameters.

2.2.2. Parameters obtained using a fitting process

The remaining parameter, λ, and initial state values $E(0)$, $I_a(0)$ and $I_s(0)$ were estimated for each locality using a curve fitting procedure to ensure that the local case data in any given jurisdiction were as close as possible to the output of the model. The fitting was done with respect to daily reports on active and cumulative cases separately, resulting in two sets of estimates for these remaining model inputs. Fitting to active cases involved comparing local active case data with the model output on $C(t)$, while fitting to cumulative cases involved comparing cumulative case numbers with the sum of all detected infections from the model, represented by the sum $\sum(\delta_a I_a + \delta_s I_s)$.

A constrained L-BFGS optimization procedure (Varadhan, 2014) was used to fit model projections to the empirical time series. We specifically minimized a squared error fitness function. Model projections $C(t)$ were produced using a Runge–Kutta numerical method (Soetaert et al., 2010). As Table 1 indicates, values of $E(0)$, $I_a(0)$, $I_s(0)$, and λ were derived in this manner. Our search space for λ was limited to the interval from 0 to 0.95. While $S(0)$ and $C(0)$ are based on data particular to each locality, we chose a consistent range of 0 to 1000 for $E(0)$, $I_a(0)$, $I_s(0)$ across all areas given that this is estimating exposures near the approximate start of local transmission. At this time period, we assume it is reasonable that these compartments will reflect low absolute numbers regardless of how large the local population is.

2.3. Operational localization procedures

In view of the real-time, dynamic deployment of the FASSSTER model, we performed the parameter fitting process in a multi-scale and iterative process. We produced estimates for all 17 regions in the Philippines. We also generated projections for each region's corresponding provinces, cities, and municipalities. We updated our model outputs twice a week. We also treated values of λ and δ_s as piece-wise constant functions with different values assigned for each month to reflect the changing state of the pandemic in the Philippines as well as the improvements in the local health systems' capacity to test, treat, and isolate confirmed cases.

3. Results

Utilization of the FASSSTER model of COVID-19 in the Philippines enabled an accurate reconstruction of local outbreak dynamics and adaptive forecasting procedures to answer shifting policy questions. In this section, we highlight two core contributions of the FASSSTER model, which we synthesize as: (a) assessing past interventions, or using the model to look back; and (b) forecasting policy outcomes, or using the model to look forward.

In the results we present below, we consider findings on different scales to illustrate the flexible uses of the FASSSTER model to suit different policy needs across time and space. These include more general, national-level questions for broader interventions; as well as more targeted policies for smaller regions and provinces.

3.1. Using the model to look back: Assessing past interventions

3.1.1. Evaluation of model performance

A prerequisite for a reliable mathematical model is its ability to accurately reconstruct previously observed case trajectories. Thus, for each locality, the parameters of the FASSSTER model for COVID-19 must be calibrated so that its output, particularly the graphs corresponding to the active cases (C) and cumulative cases, is as close as possible to the actual data.

As an illustration, Fig. 2 depicts the correspondence between model outputs and recorded trends in COVID-19 cases at national and regional levels, using data updated up to the end of August 2020. We show model fit in both active and cumulative numbers of COVID-19 cases up to end of August. Note that these are not out-of-sample projections, but all directly tuned to the data with varying λ and δ_S values per month.

The sample model outputs exhibit particularly high correlation and low error relative to empirical data. Fig. 3 indicates that across all regions, model-data correlations were generally high, ranging from 0.94 to 0.99, with a mean of 0.98 and a standard deviation of 0.01 across regions. Normalized errors were likewise low, with an average discrepancy of 0.35 cases per 1000 people in the regional population, and an overall range of mean error between 0.01 to 1.65 for active cases, and up to 2.5 for cumulative cases.

3.1.2. Quantifying policy impacts

Taken together, these findings indicate the reliability of the FASSSTER model in capturing the past case trajectories when the parameters are properly calibrated. In addition, these fitted parameter values reveal insights into the dynamics of disease transmission relative to evolving public health responses at different levels of jurisdiction.

The parameter λ, in particular, which corresponds to a transmission reduction factor, may be heuristically understood as a measure of the effectiveness of targeted community quarantine policies over time. From this standpoint, one question that may be asked is thus: How effectively did community quarantine policies lower the transmission of COVID-19? While certainly, transmission reduction in any given locality depends on a complex combination of numerous factors, the parameter λ in our model numerically captures a data-driven signal
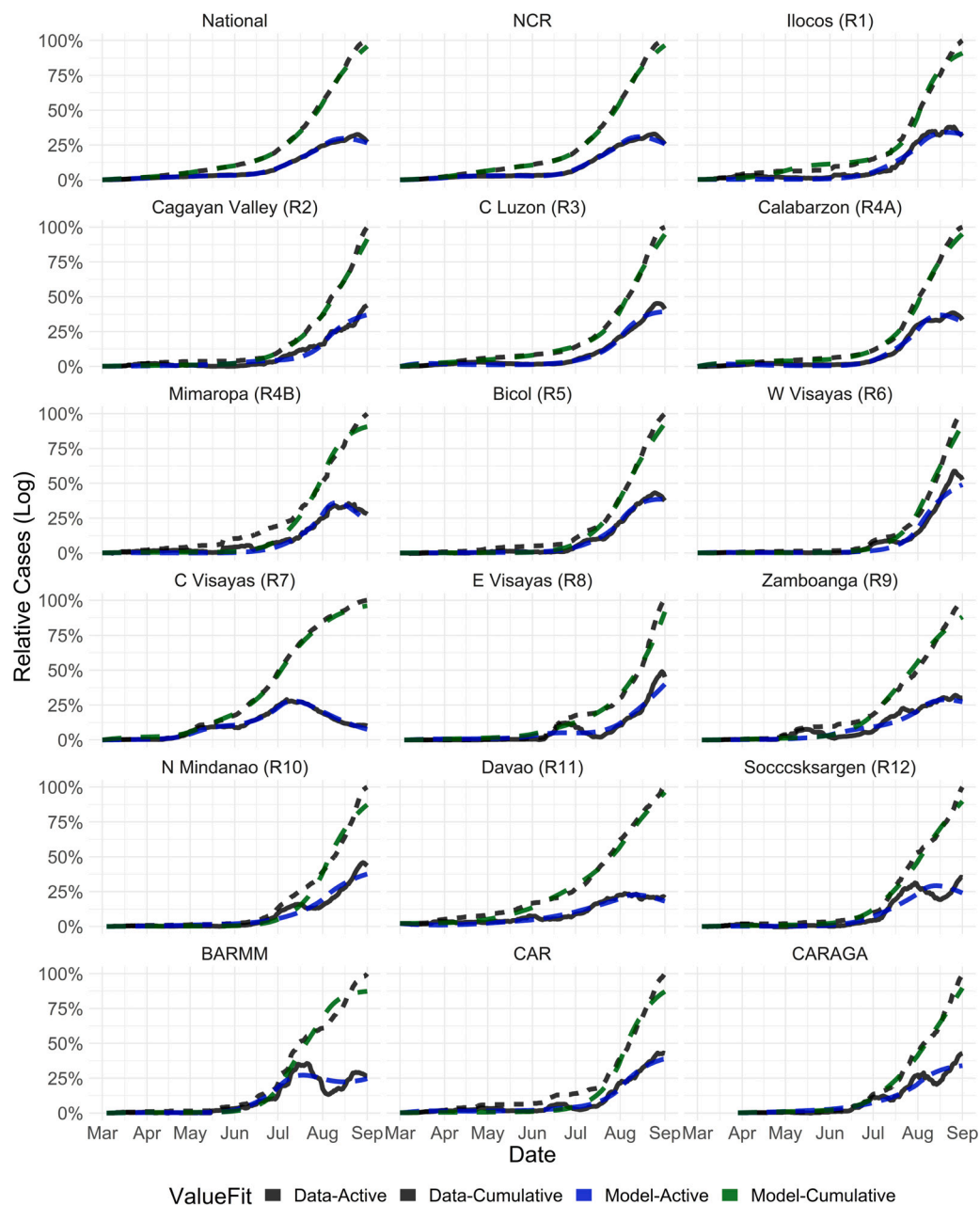
Fig. 2. Comparison of model outputs with national and regional data on active and cumulative cases. Optimized model fitting is performed iteratively on a daily basis. We present a visualization of cases normalized to the maximum incidence observed in the five-month period between the start of April to the end of August 2020.

of how disease dynamics are changing (Uyheng et al., 2018, 2020). Hence, although causal claims cannot be made solely on the basis of this parameter, it may nonetheless offer a practically useful measure that can be compared over time and space.

Fig. 4 depicts the estimated monthly values of the parameter λ in 2020 for the entire country, as well as for representative regions in the three major island groups in the Philippines: Luzon (National Capital Region), Visayas (Central Visayas Region) and Mindanao (Davao Region). National estimates of disease transmission reduction suggest the effectiveness of strict lockdown procedures implemented near the start of the pandemic, with λ values starting around values of 0.75. This corresponds to a 75% reduction in disease transmission relative to the assumed natural levels of COVID-19 transmission prior to the lockdown. However, with the easing of lockdown policies in the later months, we see that λ dips to around 0.5 in July, and rises back to around 0.6 in August.

Monthly values of λ in the National Capital Region (NCR) further appear to mirror national trends. This is understandable given that national case counts are largely driven by the infections accumulated in the capital. We observe more variability in λ in the Central Visayas Region, where an initial value close to 1 is seen in April 2020, but in alternating months, values fluctuate to as low as 0.25 in May, back to 0.75 in June, around 0.5 in July, then back above 0.75 by August. This corresponds to the similarly variable local lockdown policies, particularly in the province of Cebu, which drives most of the case counts in the region. The high variability of λ values in the Central Visayas Region suggests possibly greater region-specific sensitivity to changing lockdown policies, seeing a stronger reduction in disease transmission under restrictive policies, but also faster disease spread when restrictions are eased. These may potentially be attributed to differences in demographic distribution across populated areas, or differences in implementation and enforcement.
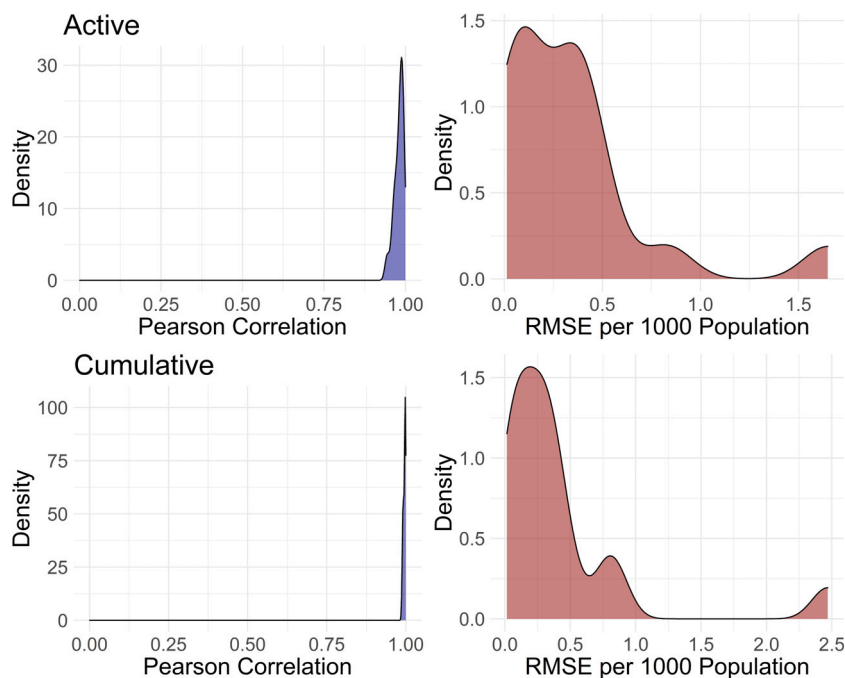
Fig. 3. Performance of models across regions for both active (top) and cumulative cases (bottom). High correlation indicates good correspondence between model output and actual data. Low root mean square error (RMSE) indicates low levels of error between model output and actual data.
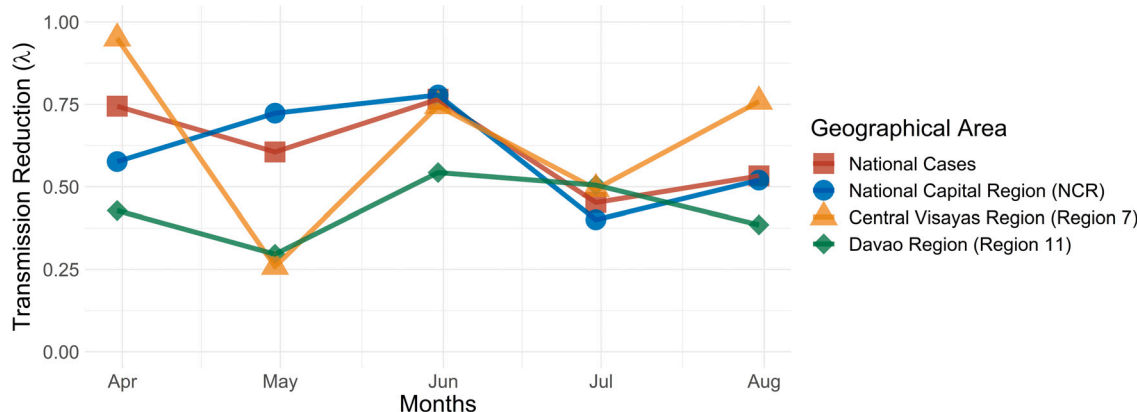

Fig. 4. Changes in monthly estimated transmission reduction λ for the year 2020. Higher values indicate more successful reduction in local spread of COVID-19. Representative regions are selected across major island groups and compared with national estimates.

Finally, we see that λ values in Davao are the most stable in the figure. Although they are initially weaker than the other regions shown, transmission reduction levels in Davao hold steady between 0.4 and 0.5, indicating relatively consistent implementation of control measures to slow local outbreak trajectories.

Taken together, these results thus illustrate the utility of the FASS-STER model for quantitative assessments of past interventions. Although different regions of the Philippines may feature different geographic and demographic contexts, parameter estimates on the model enable meaningful comparisons of policy effectiveness based on interpretable changes to disease transmission dynamics. Although not strictly defined to be the effect of lockdown policies per se, the estimated λ values nonetheless quantify concurrent changes in the rate of disease transmission, which may help policy-makers design future targeted interventions in different regions.

3.2. Using the model to look forward: Forecasting policy outcomes

Alongside assessing past interventions, the FASSSTER model has also been used to prospectively forecast future numbers of cases depending on various policy decisions. This section tackles different policy questions raised at various national and regional levels during different junctures of the Philippines' experience with the COVID-19 pandemic. We show how different answers to these policy questions could be weighed and influenced through analyzing different scenarios with the FASSSTER model, and in turn, how the FASSSTER model was adapted to meet evolving policy needs.

3.2.1. Case 1: What are the potential consequences of exiting the enhanced community quarantine?

In March 2020, the Philippine government implemented what was known as an "enhanced community quarantine" or ECQ in major regions shortly after detecting the first local transmission of COVID-19.

Table 2
Scenarios for the partial lifting of ECQ in NCR. Dates are all for the year 2020.

Factors	Scenario 1	Scenario 2	Scenario 3	Scenario 4
Start of GCQ	May 16	May 31	May 16	May 31
End of GCQ	Dec. 31	Dec. 31	Dec. 31	Dec. 31
People allowed to go out	50%	50%	50%	50%
Health system capacity (δ_S) from May 16	20%	20%	50%	50%
Estimated peak infection	170,166	159,238	22,325	18,405
Estimated peak date	Jul 20, 2020	Aug 14, 2020	May 29, 2020	May 23, 2020
Critical cases at peak date	10,210	9,554	1,339	1,104

Population mobility was severely restricted in these areas and economic activity was limited to essential services.[2]

During this ECQ, a national data analytics advisory group was formed and convened to discuss possible scenarios and generate corresponding projections that would serve as a guide in crafting policy guidelines. One of the first major policy questions was: How can the country exit the ECQ? In response, the FASSSTER model was used to analyze the effect of lifting the ECQ at different estimated levels of health system capacity. The underlying rationale behind this approach was that severe restrictions could not be sustained indefinitely, yet at the same time, public health measures needed to be in place to ensure timely detection and isolation of cases to control the spread of the disease should restrictions be gradually lifted.

From a modeling standpoint, a new parameter γ was introduced in the model to account for the percentage of the population allowed to resume pre-quarantine levels of activity, as a general proxy for easing ECQ restrictions. This resulted in an effective transmission rate of $\beta = \beta_0(1 - \lambda(1 - \gamma))$. In generating forecasts, λ is presumed to be the level of transmission reduction achieved during the ECQ period, and gamma, in turn, reduces that factor—this represents an easing in ECQ restrictions which may re-introduce higher rates of disease transmission. At the same time, the parameter δ_S was likewise varied to consider different improvements in national capacities to test, isolate, and treat COVID-19 patients.

To consider the outcomes of different levels of eased community quarantine measures, the FASSSTER model was used to generate output for different scenarios adjusting γ and δ_S. Table 2 shows a sample output of the model presenting four scenarios transitioning from ECQ to what became known as a "generalized community quarantine" (GCQ) with specific assumptions on the percentage of population resuming pre-quarantine mobility and varying health system capacity for NCR. During this time, the cases in NCR accounted for more than 70% of all the cases in the country.

Considering several factors including case projections, the Philippine government announced an initial transitional lockdown policy referred to as modified ECQ (MECQ) in NCR and selected areas. This was temporarily implemented from May 16 to 31, 2020,[3] which was then relaxed to GCQ beginning June 1, 2020.

3.2.2. Case 2: What are the potential implications of phased easing of community quarantine policies?

From this point, while the easing of ECQ allowed for economic activity to resume, a subsequent rise in COVID-19 cases and deaths began to place increasing strain on the overall health system. Beginning August 4, 2020, the quarantine status of NCR, along with neighboring provinces, was re-escalated to a modified ECQ (MECQ) for a period of two weeks. Thereafter, the government considered either extending the MECQ or reverting to GCQ in those areas. The FASSSTER model was again used to forecast the number of cases until the end of September under different scenarios.

Table 3 shows a sample output of active case projections for NCR. The value of λ used for GCQ was based on the June estimate since NCR was under GCQ for that particular month; for MECQ, the value of λ was the one fitted to August data. In this case, λ quantified the level of transmission reduction achieved by the most recent community quarantine policy. Three values of parameter δ_S, representing the health system capacity, were also considered. The results showed that returning to GCQ would be possible, provided that the health system capacity was at a sufficient level.

As in the first case, the FASSSTER model was employed to harness the optimal level of health system capacity and mobility for easing restrictions. But instead of a one-time exit from a severe ECQ, the FASSSTER model was used to consider finer-grained variations that would allow for different gradations of economic activity given different targets for improved health system capacity. This became a primary and sustained use case for the FASSSTER model in the first year of the COVID-19 pandemic.

3.2.3. Case 3: How can minimum public health standards be introduced for adequate protection while returning to sustainable levels of economic activity?

By late September in 2020, the Philippines had been under various levels of lockdown due to the pandemic for over six months. At this point, the government considered a potential scenario for fully lifting quarantine measures under a "New Normal" (NN) arrangement. Here, the primary consideration was returning to sustainable levels of activity in view of a medium-term to a long-term continuation of the pandemic while access to vaccinations remained uncertain at the time. The proposed New Normal policy would target areas where the number of new cases over the last 2 weeks was either zero or below a specified threshold. Another option for these areas was modified GCQ (MGCQ), under which almost 80% of the population could resume pre-quarantine mobility.

In considering these policies, the government considered the stricter enforcement of minimum public health standards (MPHS) such as physical distancing of at least 1 meter, wearing face masks and face shields, and proper hand hygiene, as a viable alternative to community quarantine. For instance, wearing of face masks and face shields in public places became mandatory in mid-August 2020 for NCR. Post-implementation showed that the disease transmission rate significantly declined, as seen in the high value of λ obtained when the August data were fitted to the model.

Table 4 shows sample projections for the province of Albay in the Bicol Region, considered as a low-risk area, under two community quarantine policies, New Normal and MGCQ, for the months of October and November 2020. Note that Albay had been under MGCQ since June 2020. Because multiple values for λ were now available to use, simulations used both the smallest and largest values of λ in previous months. This produced a range of projected cases for each date.

Under the New Normal scenario, we obtained the corresponding values of λ by taking 25% of the MGCQ values. This was based on the assumption that if, on average, MGCQ represented restrictions on activity for 20% of the population, the New Normal would only restrict activities for about 5% of the population (hence, 25% of the MGCQ value). Compliance with the MPHS, especially in public places, was assumed to reduce the transmission rate by 85% (Chu et al.,

Table 3
Projections of the cumulative cases in NCR under GCQ and MECQ. Dates are all for the year 2020.

Date	GCQ after Aug 18			MECQ to Aug 31, GCQ from Sep 1		
	$\delta_S = 25\%$	$\delta_S = 35\%$	$\delta_S = 50\%$	$\delta_S = 25\%$	$\delta_S = 35\%$	$\delta_S = 50\%$
Aug 31	129,383	130,116	129,826	127,468	128,489	128,596
Sep 15	168,766	154,180	143,382	146,296	140,512	135,964
Sep 30	218,547	172,367	149,278	166,531	148,065	138,641

Table 4
Projected cumulative cases in the province of Albay under MGCQ and New Normal. Dates are all for the year 2020.

	MGCQ			New Normal		
Date	0% Comp.	30% Comp.	50% Comp.	0% Comp.	30% Comp.	50% Comp.
Oct 15	932–953	926–941	923–934	958–964	945–949	937–940
Oct 31	1001–1136	974–1046	959–1004	1179–1239	1067–1095	1017–1033
Nov 15	1047–1403	995–1141	971–1048	1551–1782	1193–1269	1073–1107
Nov 30	1080–1810	1006–1232	976–1078	2205–2895	1330–1485	1115–1170

Table 5
Community quarantine scenarios in NCR+ from March 29 to May 15. Dates are all for the year 2021.

Scenario	March 29–April 4	April 5–11	April 12–18	April 19–May 15
Scenario 1	ECQ	MECQ	MECQ	GCQ
Scenario 2	ECQ	GCQ	GCQ	GCQ
Scenario 3	ECQ	ECQ	MECQ	MECQ
Scenario 4	ECQ	ECQ	MECQ	GCQ
Scenario 5	ECQ	ECQ	GCQ	GCQ
Scenario 6	ECQ	ECQ	ECQ	MECQ
Scenario 7	ECQ	ECQ	ECQ	GCQ
Scenario 8	ECQ	ECQ	ECQ	ECQ

2020). Compliance rate represents the percentage of the population who practice MPHS. We revised the transmission rate in the model as $\beta = \beta_0(1-\lambda)(1-\kappa\eta)$, where $\kappa = 0.85$, η represents the MPHS compliance rate and $\kappa\eta \in [0, 1)$. Lastly, the value of δ_s in all scenarios was set at 19%, based on the September case data.

3.2.4. Case 4: How can reimplementation of community quarantine policies mitigate surges in new cases?

In the months that followed, the pandemic seemed to have remained within manageable levels in most parts of the country, even during the holiday season from December 2020 to early January 2021. As such, travel restrictions to and from different regions and provinces were relaxed.[4] However, in mid-March 2021, the number of cases was observed to have started to rise especially in NCR and some cities and provinces in the neighboring Calabarzon region. This prompted the national government to declare these parts of the country, referred to as NCR+, under a bubble beginning March 22.

This policy meant that NCR+ would remain under GCQ but residents were restricted from exiting the bubble and non-residents would not be allowed in. This measure, however, did not stop the surge in the number of cases, resulting in a huge burden on the health system capacity. It was also at this time that results of the genome sequencing studies confirmed the presence of new variants in the country.[5] The new variants were now added to the list of possible causes of increase in cases, alongside relaxation of movement in the population. Hence, the national government imposed the strictest community quarantine policy, ECQ, in NCR+ from March 29 to April 11. The policy shifted to a less stringent MECQ beginning April 12 taking into account economic losses, then to GCQ beginning May 15 when the number of cases seemed to have become manageable.

---

[4] https://doh.gov.ph/sites/default/files/health-update/IATFResolution101.pdf.

[5] https://doh.gov.ph/sites/default/files/health-update/IATFResolution106.pdf.

Fig. 5 shows a sample output of the FASSSTER model generated on March 31, 2021 based on different scenarios of varying community quarantine policies (CQ) in NCR+ from March 29 to May 15, as described in Table 5. The projections per CQ policy were obtained by specifying the transmission rate β whose components were derived according to the scenario being considered. This time, we reformulated β to capture both varying mobility and MPHS compliance and used the formula $\beta = \beta_0(1 - \lambda)$, where $(1 - \lambda) = (1 - \Lambda(1 - \gamma))(1 - \kappa\eta)$. The parameter $\gamma \in [0, 1]$ represents the population mobility as estimated from Google mobility data, η is the level of compliance of the general population to MPHS, $\kappa = 0.85$, $\kappa\eta \in [0, 1)$, and Λ is a constant (per locality) calculated from the April 2020 values of λ and γ with the assumption that the MPHS compliance rate $\eta = 0$ up to that month (since this is the early stage of the pandemic). The monthly values of λ up to March 31, 2021 were those fitted to the historical case data. For the projections, the value of λ was calculated per week using the preceding formula with γ equal to the average mobility level when a specified CQ was previously in place and the MPHS compliance rate η was assumed to have a proportionate improvement from the previous month's computed value. Ultimately, the decision was to impose ECQ in NCR+ up to April 11. For the succeeding weeks, projections were updated using the most recent data and these, together with economic considerations, provided guidance for the CQ policies imposed.

4. Discussion

In conjunction with relevant socio-economic and security indicators, the FASSSTER model served as a useful tool in evaluating policy options to address regional needs for pandemic response. Conversely, the model has adapted to changing policies by introducing new parameters that would capture new questions raised in the evolving policy context of controlling the spread of the disease. Table 6 summarizes the timeline of how and why the model was used at different policy-making junctures.

From March to April 2020, when local cases were below 4,000, the model was used mainly to understand the spread of the disease, including its forecasted peak, and eventual total cases and mortalities. From May to June, economic costs precipitated new guidance on easing mobility restrictions in accordance with the current and target health system capacity, prompting model adjustments to account for such changes in policy. From July 2020 until the first half of March 2021, scenario analysis determined how stricter enforcement of MPHS and enhanced health system capacity to test, isolate, and treat patients in both hospitals and community care facilities could serve as viable alternatives to community-wide lockdowns. Finally, when the number of cases surged in the second half of March 2021, the model was once again employed to guide policy-makers in determining interventions that would control further spread of the disease.
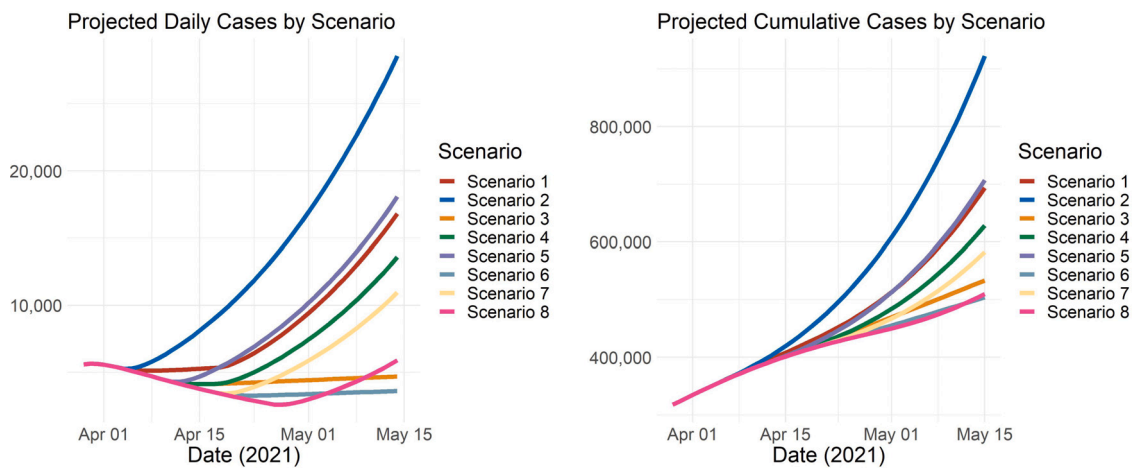
Projected Daily Cases by Scenario

Projected Cumulative Cases by Scenario

Fig. 5. Projections of daily new cases and cumulative cases in NCR+ for March 29 to May 15, 2021 corresponding to each scenario. The daily case projections is derived from the projections on cumulative cases.

Table 6
Timeline of model applications in policy-making.

Phase	Purpose	Use of the Model	Policy Implication
Phase 1 (March–April 2020)	Understanding the local spread of COVID-19 in NCR and other regions	Projection of the peak of the epidemic curve Projection of the total numbers of cases and disease-related deaths	Effectiveness of community quarantine, augmentation of resources[a]
Phase 2 (May–June 2020)	Easing of lockdown restrictions	Introducing a transmission rate multiplier to account for targeted gradual increase in population mobility Scenario analysis using different values of the parameter δ_s which represents the health system capacity	More relaxed community quarantine policies depending on the health and economic risk status of a locality; partial opening of business establishments; workers in certain sectors allowed to go back to work Improvements to health system capacity, particularly the increase in testing[b]
Phase 3 (July 2020 to mid-March 2021)	Finding alternatives to community quarantine Continuous monitoring of case trajectories	Scenario analysis using adjustments in the past monthly values of disease transmission rates combined with different values of δ_s	Opening up of the economy by relaxing community quarantine policies Stricter enforcement of health protocols, higher targets for testing and isolation, intensified contact tracing efforts[c]
Phase 4 (mid-March to June 2021)	Determining the appropriate community quarantine policies brought about by the surge in case numbers	Transmission rate corresponding to each community quarantine policy adjusted to account for three factors: the presence of new variants, mobility, and compliance to health protocols	Changing community quarantine policies, from strict to more relaxed policies, in response to changing case trajectories

[a] https://doh.gov.ph/sites/default/files/health-update/IATF-RESO-15.pdf.
[b] https://doh.gov.ph/sites/default/files/health-update/IATF-Resolution-No.-50.pdf.
[c] https://doh.gov.ph/sites/default/files/health-update/IATFResolution60A.pdf.

A vast literature tackles the general design and calibration of mathematical models for understanding the outbreak dynamics of COVID-19 in general, or to answer specific policy questions in an abstract setting of inquiry (Eikenberry et al., 2020; Gnanvi et al., 2021; Lin et al., 2020b,a; Rahimi et al., 2021; Syeda et al., 2021; Wynants et al., 2020). In this paper, we detail both the mathematical framework for understanding COVID-19 in the Philippines, as well as how it was used to answer multiple, concrete, and shifting policy questions over time (Estuar et al., 2020; Vallejo and Ong, 2020). Moreover, we demonstrate the reciprocal relationship between substantive policy concerns with the design, deployment, and dynamic evolution of mathematical modeling techniques. An effective COVID-19 model requires constant

adjustments because of the volatile knowledge base around the novel pathogen. Such information asymmetries compound existing resource constraints of a developing country like the Philippines, and further highlight the utility and necessity of data-driven bases for controlling disease spread and crisis analytics in general (Cattani, 2020; Dahab et al., 2020; Figueroa et al., 2021; McMahon et al., 2020). Tight and responsive coupling between emergent pandemic challenges and computational modeling efforts likewise facilitates the formalization of policy questions into more precise evaluations of simulated outcomes, timely what-if analyses of counterfactual scenarios, as well as innovation of new policy measures based on model insights.

However, limitations of the FASSSTER model – in terms of *both* its mathematical and policy-interface dimensions – are also important to take into consideration. From the standpoint of the model, we did not account for reinfections nor new variants of the pathogen that may potentially explain the high number of daily new cases that have emerged to date (Gousseff et al., 2020). Seasonal changes were also not incorporated into the model, which may affect the early identification of suspect COVID-19 cases (Liu et al., 2021). As noted in international experiences, data quality issues and fluctuating capacity limits on public testing also suggest caution in extrapolating the true number of cases outside formal detection mechanisms in the country (Sáez et al., 2021). Key considerations also nuance the interpretation of parameter estimates, such as λ, which may heuristically capture data-driven changes in disease transmission associated with policy measures, but may not be exclusively explained by such interventions. Similarly, assuming the detection rate for asymptomatic individuals (δ_a) to be equal to the detection rate for symptomatic individuals (δ_s) may likely be an overestimation due to the different testing approaches for the two groups. For example, some government-initiated programs prioritize testing symptomatic individuals (Kabagani, 2022; Magsambol, 2022). This consequently may lead to a partitioning of confirmed cases into symptomatic and asymptomatic different from the actual data although the totality will be the same because the model is fitted primarily to the number of confirmed cases regardless of their clinical status. Other factors are always at play in complex systems like pandemics, which the FASSSTER model does not comprehensively incorporate into its design.

On the policy side, we also affirm the importance of other science-policy interfaces that differ from those detailed by the FASSSTER case in the Philippines (Estuar et al., 2020). For instance, the organizational structure and composition of other pandemic advisory bodies like SAGE in the United Kingdom may feature their own set of advantages and disadvantages relative to the local context (Freedman, 2020; Vallejo and Ong, 2020). This work does not aim to normatively prescribe a universal model of policy-driven mathematical modeling, but rather descriptively document the singular experience of FASSSTER in the Philippines. To this end, we observe that at the time of writing, significant challenges remain with respect to quelling the ravages of the pandemic in the Philippines, and recognize that model forecasts and simulations represent merely one component of a larger public health system embedded in complex issues of resource allocation, policy implementation, collective behavior, and multiple levels of local and global leadership (Chiriboga et al., 2020; Mendenhall, 2020; Montiel et al., 2021; Van Bavel et al., 2020).

5. Conclusion

In conclusion, the FASSSTER compartmental model was reliable in projecting local COVID-19 case trajectories and trends in the Philippines. For this reason, it provided an effective tool in policy design for pandemic response in the Philippines. Central to the sustained value of the FASSSTER model to evolving policies and pandemic conditions were efforts to adapt to new policy needs and the shifting availability of data.

Although initial control measures in the form of widespread community quarantines were effective in the short term, their pervasive effects on the economy posed new questions for policy-makers. Over time, the FASSSTER model provided data-driven support for the implementation of policies related to the rigorous enforcement of MPHS, continuous increases in health system capacity, and improvements in early case detection and isolation efforts. These factors continue to be measured and compared with scenario analysis outputs in the FASSSTER model.

At the time of writing, the Philippines has entered a new phase of the pandemic where the detection of variants of concern (VOC) is increasing. At the same time, the country has also started its vaccination program. The FASSSTER model continues to consider and incorporate these developments into its design, highlighting the ongoing importance of policy-driven mathematical modeling in response to imminent and unforeseen crises.

CRediT authorship contribution statement

Elvira de Lara-Tuprio: Conception and design of the work, Design of the SEIR model, Parameter estimation, Simulation analysis, Writing – original draft. **Carlo Delfin S. Estadilla:** Design of the SEIR model, Parameter estimation, Simulation analysis, Writing – original draft. **Jay Michael R. Macalalag:** Design of the SEIR model, Parameter estimation, Simulation analysis, Writing – original draft. **Timothy Robin Teng:** Design of the SEIR model, Parameter estimation, Simulation analysis, Writing – original draft. **Joshua Uyheng:** Design of the SEIR model, Parameter estimation, Simulation analysis, Writing – original draft. **Kennedy E. Espina:** Acquisition of the data, Writing – original draft. **Christian E. Pulmano:** Acquisition of the data, Writing – original draft. **Maria Regina Justina E. Estuar:** Conception and design of the work, Acquisition of the data, Writing – original draft. **Raymond Francis R. Sarmiento:** Acquisition of the data, Design of the SEIR model, Parameter estimation, Simulation analysis, Writing – original draft.

Declaration of competing interest

The authors declare that they have no known competing financial interests or personal relationships that could have appeared to influence the work reported in this paper.

References

Bedford, Juliet, Enria, Delia, Giesecke, Johan, Heymann, David L., Ihekweazu, Chikwe, Kobinger, Gary, Lane, H. Clifford, Memish, Ziad, Oh, Myoung-don, Schuchat, Anne, et al., 2020. COVID-19: Towards controlling of a pandemic. Lancet 395 (10229), 1015–1018.

Boccaletti, Stefano, Ditto, William, Mindlin, Gabriel, Atangana, Abdon, 2020. Modeling and forecasting of epidemic spreading: The case of COVID-19 and beyond. Chaos, Solitons, Fractals.

Cattani, Michele, 2020. Global coalition to accelerate COVID-19 clinical research in resource-limited settings. Lancet.

Chiriboga, David, Garay, Juan, Buss, Paulo, Madrigal, Rocío Sáenz, Rispel, Laetitia Charmaine, 2020. Health inequity during the COVID-19 pandemic: A cry for ethical global leadership. Lancet 395 (10238), 1690–1691.

Chu, Derek K., Akl, Elie A., Duda, Stephanie, Solo, Karla, Yaacoub, Sally, Schünemann, Holger J., El-harakeh, Amena, Bognanni, Antonio, Lotfi, Tamara, Loeb, Mark, et al., 2020. Physical distancing, face masks, and eye protection to prevent person-to-person transmission of SARS-CoV-2 and COVID-19: A systematic review and meta-analysis. Lancet.

Currie, Christine S.M., Fowler, John W., Kotiadis, Kathy, Monks, Thomas, Onggo, Bhakti Stephan, Robertson, Duncan A., Tako, Antuela A., 2020. How simulation modelling can help reduce the impact of COVID-19. J. Simul. 1–15.

Dahab, Maysoon, Van Zandvoort, Kevin, Flasche, Stefan, Warsame, Abdihamid, Ratnayake, Ruwan, Favas, Caroline, Spiegel, Paul B., Waldman, Ronald J., Checchi, Francesco, 2020. COVID-19 control in low-income settings and displaced populations: What can realistically be done? Conflict Health 14 (1), 1–6.

DebRoy, Swati, Prosper, Olivia, Mishoe, Austin, Mubayi, Anuj, 2017. Challenges in modeling complexity of neglected tropical diseases: A review of dynamics of visceral leishmaniasis in resource limited settings. Emerg. Themes Epidemiol. 14 (1), 10.

Department of Health - Epidemiology Bureau, 2020. Covid-19 tracker Philippines. https://www.doh.gov.ph/covid19tracker. Retrieved September 2020.

Eikenberry, Steffen E., Mancuso, Marina, Iboi, Enahoro, Phan, Tin, Eikenberry, Keenan, Kuang, Yang, Kostelich, Eric, Gumel, Abba B., 2020. To mask or not to mask: Modeling the potential for face mask use by the general public to curtail the COVID-19 pandemic. Infect. Dis. Model..

Espina, Kennedy, Estuar, Ma Regina Justina E., 2017. Infodemiology for syndromic surveillance of dengue and typhoid fever in the Philippines. Procedia Comput. Sci. 121, 554–561.

Estadilla, Carlo Delfin S., Uyheng, Joshua, de Lara-Tuprio, Elvira P., Teng, Timothy Robin, Macalalag, Jay Michael R., Estuar, Maria Regina Justina E., 2021. Impact of vaccine supplies and delays on optimal control of the Covid-19 pandemic: Mapping interventions for the Philippines. Infect. Dis. Poverty 10 (04), 46–59.

Estuar, Maria Regina Justina E., de Leon, Marlene, Benito, Daniel Joseph, Estadilla, Carlo, de Lara-Tuprio, Elvira, Teng, Timothy, Uyheng, Joshua, 2020. Science and public service during a pandemic: Reflections from the scientists of the Philippine government's COVID-19 surveillance platform. Philippine Stud.: Hist. Ethnogr. Viewp. 68 (3/4), 493–504.

Figueroa, J. Peter, Bottazzi, Maria Elena, Hotez, Peter, Batista, Carolina, Ergonul, Onder, Gilbert, Sarah, Gursel, Mayda, Hassanain, Mazen, Kim, Jerome H., Lall, Bhavna, et al., 2021. Urgent needs of low-income and middle-income countries for COVID-19 vaccines and therapeutics. Lancet 397 (10274), 562–564.

Freedman, Lawrence, 2020. Scientific advice at a time of emergency: SAGE and Covid-19. Political Q. 91 (3), 514–522.

Gnanvi, Janyce, Salako, Kolawolé Valère, Kotanmi, Brezesky, Kakaï, Romain Glèlè, 2021. On the reliability of predictions on COVID-19 dynamics: A systematic and critical review of modelling techniques. Infect. Dis. Model..

Gousseff, Marie, Penot, Pauline, Gallay, Laure, Batisse, Dominique, Benech, Nicolas, Bouiller, Kevin, Collarino, Rocco, Conrad, Anne, Slama, Dorsaf, Joseph, Cédric, Lemaignen, Adrien, Lescure, François-Xavier, Levy, Bruno, Mahevas, Matthieu, Pozzetto, Bruno, Vignier, Nicolas, Wyplosz, Benjamin, Salmon, Dominique, Goehringer, Francois, Botelho-Nevers, Elisabeth, 2020. Clinical recurrences of COVID-19 symptoms after recovery: Viral relapse, reinfection or inflammatory rebound? J. Infect. jun.

Kabagani, Lade Jean, 2022. Makati to provide free covid-19 tests to residents. https://www.pna.gov.ph/articles/1165653, Retrieved February 2022.

Lin, Yi-Fan, Duan, Qibin, Zhou, Yiguo, Yuan, Tanwei, Li, Peiyang, Fitzpatrick, Thomas, Fu, Leiwen, Feng, Anping, Luo, Ganfeng, Zhan, Yuewei, et al., 2020a. Spread and impact of COVID-19 in China: A systematic review and synthesis of predictions from transmission-dynamic models. Front. Med. 7, 321.

Lin, Qianying, Zhao, Shi, Gao, Daozhou, Lou, Yijun, Yang, Shu, Musa, Salihu S., Wang, Maggie H., Cai, Yongli, Wang, Weiming, Yang, Lin, et al., 2020b. A conceptual model for the coronavirus disease 2019 (COVID-19) outbreak in Wuhan, China with individual reaction and governmental action. Int. J. Infect. Dis. 93, 211–216.

Liu, Xiaoyue, Huang, Jianping, Li, Changyu, Zhao, Yingjie, Wang, Danfeng, Huang, Zhongwei, Yang, Kehu, 2021. The role of seasonality in the spread of COVID-19 pandemic. Environ. Res. 195, 110874.

macrotrends, 2020a. Philippines birth rate 1950–2020. https://www.macrotrends.net/countries/PHL/philippines/birth-rate. Retrieved August 2020.

macrotrends, 2020b. Philippines life expectancy 1950–2020. https://www.macrotrends.net/countries/PHL/philippines/life-expectancy. Retrieved August 2020.

Magsambol, Bonz, 2022. Doh wants symptomatic, vulnerable patients prioritized for covid-19 testing. https://www.rappler.com/nation/department-health-wants-covid-19-testing-limited-symptomatic-patients-vulnerable-groups/. Retrieved February 2022.

McMahon, Devon E., Peters, Gregory A., Ivers, Louise C., Freeman, Esther E., 2020. Global resource shortages during COVID-19: Bad news for low-income countries. PLoS Negl. Trop. Dis. 14 (7), e0008412.

Mendenhall, Emily, 2020. The COVID-19 syndemic is not global: Context matters. Lancet 396 (10264), 1731.

Mizumoto, Kenji, Kagaya, Katsushi, Zarebski, Alexander, Chowell, Gerardo, 2020. Estimating the asymptomatic proportion of coronavirus disease 2019 (COVID-19) cases on board the diamond princess cruise ship, Yokohama, Japan, 2020. Eurosurveillance 25 (10), mar.

Montiel, Cristina Jayme, Uyheng, Joshua, Paz, Erwine Dela, 2021. The language of pandemic leaderships: Mapping political rhetoric during the COVID-19 outbreak. Political Psychol..

Philippine Statistics Authority, 2020. Census of population and housing. https://psa.gov.ph/population-and-housing.

Prem, Kiesha, Liu, Yang, Russell, Timothy W., Kucharski, Adam J., Eggo, Rosalind M, Davies, Nicholas, Flasche, Stefan, Clifford, Samuel, Pearson, Carl A.B., Munday, James D., et al., 2020. The effect of control strategies to reduce social mixing on outcomes of the COVID-19 epidemic in Wuhan, China: A modelling study. Lancet Public Health.

Rahimi, Iman, Chen, Fang, Gandomi, Amir H., 2021. A review on COVID-19 forecasting models. Neural Comput. Appl. 1–11.

Sáez, Carlos, Romero, Nekane, Conejero, J. Alberto, García-Gómez, Juan M., 2021. Potential limitations in COVID-19 machine learning due to data source variability: A case study in the NCov2019 dataset. J. Am. Med. Inform. Assoc. 28 (2), 360–364.

Soetaert, Karline, Petzoldt, Thomas, Setzer, R. Woodrow, 2010. Package desolve: Solving initial value differential equations in r. J. Stat. Softw. 33 (9), 1–25.

Stokel-Walker, Chris, 2021. What we know about covid-19 reinfection so far. Bmj 372.

Syeda, Hafsa Bareen, Syed, Mahanazuddin, Sexton, Kevin Wayne, Syed, Shorabuddin, Begum, Salma, Syed, Farhanuddin, Prior, Fred, Yu, Jr., Feliciano, 2021. Role of machine learning techniques to tackle the COVID-19 crisis: Systematic review. JMIR Med. Inform. 9 (1), e23811.

U.S. Centers for Disease and Control, 2020. COVID-19 pandemic planning scenarios. https://www.cdc.gov/coronavirus/2019-ncov/hcp/planning-scenarios.html. Retrieved August 2020.

Uyheng, Joshua, Pulmano, Christian E., Estuar, Ma Regina Justina, 2020. Deploying system dynamics models for disease surveillance in the philippines. In: International Conference on Social Computing, Behavioral-Cultural Modeling and Prediction and Behavior Representation in Modeling and Simulation. pp. 35–44, Springer.

Uyheng, Joshua, Rosales, John Clifford, Espina, Kennedy, Estuar, Ma Regina Justina, 2018. Estimating parameters for a dynamical dengue model using genetic algorithms. In: Proceedings of the Genetic and Evolutionary Computation Conference Companion. pp. 310–311.

Vallejo, Jr., Benjamin M., Ong, Rodrigo Angelo C., 2020. Policy responses and government science advice for the COVID-19 pandemic in the Philippines: January to April 2020. Progr. Disaster Sci. 7, 100115.

Van Bavel, Jay J., Baicker, Katherine, Boggio, Paulo S., Capraro, Valerio, Cichocka, Aleksandra, Cikara, Mina, Crockett, Molly J., Crum, Alia J., Douglas, Karen M., Druckman, James N., et al., 2020. Using social and behavioural science to support COVID-19 pandemic response. Nat. Hum. Behav. 4 (5), 460–471.

Varadhan, Ravi, 2014. Numerical optimization in R: Beyond optim. J. Stat. Softw. 60 (1), 1–3.

World Health Organization, 2020a. Coronavirus disease 2019 situation report-73. https://www.who.int/docs/default-source/coronaviruse/situation-reports/20200402-sitrep-73-covid-19.pdf. Retrieved September 2020.

World Health Organization, 2020b. Report of the WHO-China joint mission on coronavirus disease 2019 (COVID-19). https://www.who.int/docs/default-source/coronaviruse/who-china-joint-mission-on-covid-19-final-report.PDF.

Wynants, Laure, Calster, Ben Van, Collins, Gary S., Riley, Richard D., Heinze, Georg, Schuit, Ewoud, Bonten, Marc M.J., Dahly, Darren L., Damen, Johanna A.A., Debray, Thomas P.A., et al., 2020. Prediction models for diagnosis and prognosis of COVID-19: Systematic review and critical appraisal. BMJ 369.